Bioconjugate Chemistry

Article

pubs.acs.org/bc

Polyethylene Glycol Modified FGF21 Engineered to Maximize Potency and Minimize Vacuole Formation

Jing Xu,[†] Jeanine Bussiere,[‡] Junming Yie,[†] Allen Sickmier,[∥] Phil An,[§] Ed Belouski,[§] Shanaka Stanislaus,[†] and Kenneth W. Walker*[,§]

[†]Department of Metabolic Disorders, [‡]Department of Comparative Biology and Safety Sciences, [∥]Department of Molecular Structure and Characterization, and [§]Department of Biologics, Amgen Inc., One Amgen Center Drive, Thousand Oaks, California 91320, United States

ABSTRACT: Fibroblast growth factor 21 (FGF21) is involved in regulating energy metabolism, and it has shown significant promise as a treatment for type II diabetes; however, the native protein has a very short circulating half-life necessitating frequent injections to maintain a physiological effect. Polyethylene glycol (PEG) conjugation to proteins has been used as a method for extending the circulating half-life of many pharmaceutical proteins; however, PEG does carry the risk of vacuole formation, particularly in the renal tubular epithelium. Since renal vacuole formation may be particularly problematic for diabetic patients, we engineered site-directed PEGylated variants of FGF21 with sustained potency and minimized vacuole formation. This was accomplished both by probing the site of PEGylation on FGF21 as well as by examining various PEG configurations. While the site of PEGylation has a significant impact on the bioactivity of FGF21, it has only a marginal impact on vacuole formation; however, the configuration and number of PEGs conjugated to the protein has a much more profound effect on vacuologenesis.

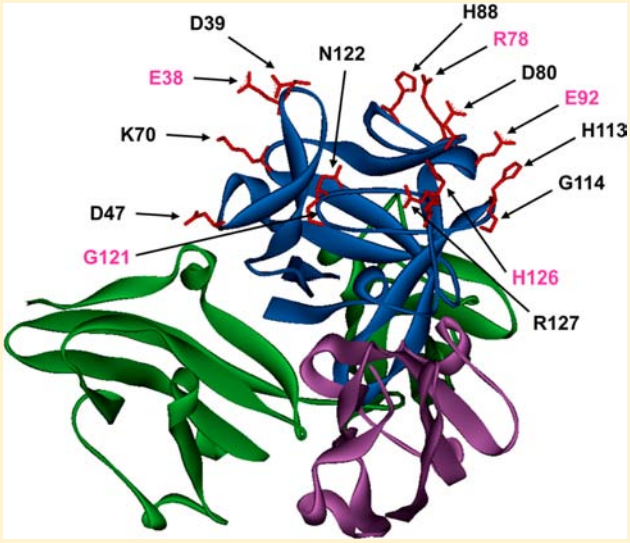

INTRODUCTION

Although a number of antidiabetic drugs are available on the market, most of the drugs fail to provide adequate glycemic control as type 2 diabetes progresses.[1] FGF21 is a promising protein therapeutic alternative to insulin and GLP1 analogues for the treatment of type 2 diabetes. FGF21, along with FGF19 and FGF23, are members of a subclass of the FGF family,[2] which are pivotal in the maintenance of physiological homeostasis related to metabolism.[3] FGF19 is critical for the regulation of bile acid metabolism, FGF23 for phosphate and vitamin D metabolism, and FGF21 for glucose, lipid, and energy homeostasis.[4−6]

FGF21 is a 20 K_d secreted protein preferentially expressed in the liver, pancreas, and adipose tissues, and its expression is metabolically regulated.[7] Upon secretion, FGF21 binds to a membrane-bound coreceptor, β-klotho, and selectively activates FGFR c-isoforms in metabolic tissues.[8] FGF21 has been shown to be a regulator of cellular metabolism and to exert a beneficial pleiotropic effect *in vitro* and *in vivo*, suppressing hepatic glucose production, stimulating adipose tissue glucose uptake, increasing brown adipose tissue thermogenesis, and preserving pancreatic islet mass and insulin content.[9−11] In diabetic rodent models, administration of FGF21 acutely lowers blood glucose levels and improves insulin sensitivity.[11] Chronic treatment with FGF21 in rodents and monkeys also decreases blood and tissue triglyceride levels, total cholesterol and LDL-cholesterol, while raising HDL-cholesterol levels in monkeys.[12,13] FGF21 also shows a potent weight loss effect and has potential as an antiobesity therapeutic.[9,12,14]

We previously described an Fc-fused FGF21 analog that exhibited favorable pharmaceutical attributes compared to native human FGF21. These attributes included prolonged pharmacokinetic and phamacodynamic profiles, enhanced efficacy, and a resistance to *in vitro* aggregation and *in vivo* proteolytic degradation.[15] Here we describe the development of PEG conjugated-FGF21 as an alternative strategy to improve the pharmacokinetics and pharmacodynamics of the protein and to enable a more convenient dosing regimen. PEG is frequently conjugated to proteins in order to enhance their pharmacokinetic and/or solubility profile because of its high solubility, low toxicity, and low immunogenicity;[16−19] however, PEG is associated with the accumulation of intracellular vacuoles, which have unknown biological consequences.[20,21] Accumulation of PEG associated vacuoles in the proximal tubules of the renal epithelium is of particular concern in patient populations that have a high incidence of renal failure, such as diabetics. For these reasons, a structure based engineering approach was employed to rationally

Received: November 12, 2012
Revised: April 16, 2013
Published: April 18, 2013

identify optimized sites for PEG attachment to FGF21. This was followed by an examination of the effect of PEG configuration on the vacuole-forming potential of various PEGylated FGF21 molecules to identify candidates that were potent *in vivo*, produced low levels of vacuoles, and were efficient to produce.

EXPERIMENTAL PROCEDURES

Homology Model. The FGF21 homology model was prepared using Modeler in Discovery studio 3.0 (Accelrys) with FGF19 (PDB code: 2P23) used as a template. The program Coot was used to manually place FGF21 into a complex with the fibroblast growth factor receptor 1 using the FGF2-FGFR1-Heparin complex (PDB code: 1FQ9) as a guide.[23]

Cell Lines and Protein Expression. *E. coli* strain BL21Star (DE3) obtained from Invitrogen was used as a host organism. Wild-type, human, mature FGF21 (29−209, without signal peptide) (MHPIPDSSPLLQFGGQVRQRYLYTDDAQQ-TEAHLEIREDGTVGGAADQSPESLLQLKALKPGVI-QILGVKTSRFLCQRPDGALYGSLHFDPEACSFRELL-LEDGYNVYQSEAHGLPLHLPGNKSPHRDPAPRG-PARFLPLPGLPPAPPEPPGILAPQPPDVGSSDPLSMVGPS-QGRSPSYAS) was amplified by PCR from a cDNA clone and ligated between NdeI and *Eco*RI sites in pET30 (Merck Millipore) and then transformed into competent cells. Underlined residues were mutated to cysteine one at a time and bolded residues were paired for dual-pegylation constructs.

Mutagenesis was achieved with a modified whole-plasmid amplification protocol. Only the first 15 nucleotides of the primer pairs, including the mutated codon(s), were complementary. For example, plus strand oligo atcagggag**tgc**gggacggtgggggc and minus oligo ccc**gca**ctccctgatctccaggtgggc were used to generate the D39C variant. Amplification products were digested with the restriction endonuclease DpnI, and then transformed into competent cells. Coding regions were sequenced to confirm the absence of polymerase-generated errors. Two rounds were required for mutations more than approximately five residues apart.

One-liter bottles of Terrific Broth (Teknova) media were directly inoculated with expression strains. The bottles were tightly capped and incubated, without shaking, overnight at 37 °C. Anoxic conditions lead to cell growth halting at OD600−1.3. The next morning, 0.5 L aliquots were transferred to two beveled flasks (2.5 L). The flasks were shaken at 400 rpm and 37 °C for half an hour prior to induction to allow the culture to recover. Inductions were performed using isopropyl β-D-1-thiogalactopyranoside (0.1 mM final concentration) (Calbiochem, San Diego, CA) after recovery and expression was continued overnight.

Protein Purification and Analysis. All reagents used for purification and analysis were obtained from Sigma Aldrich (St. Louis, MO) unless otherwise noted. The cell paste was homogenized in four volumes of water and the cells were disrupted using a microfluidizer at 16 000 PSI. The lysate was centrifuged at 5000 *g* for 45 min to pellet the inclusion bodies (IBs) and the resulting supernatant was decanted to waste. The pellet was rehomogenized using half the original volume of water, centrifuged, and the supernatant decanted. These 3 steps were repeated once more to achieve double-washed IBs (dwIBs). The dwIBs were stored at −80 °C.

The frozen dwIBs were solubilized in a 1:4, weight to volume, ratio of 50 mM tris, 7.5 M urea (Amresco, Solon, OH), 1 M GnHCl (Teknova, Hollister, CA), 12.5 mM DTT, pH 9.0, and then gently stirred at room temperature for 1 h. The solubilized dwIBs were refolded in a 1:25 ratio of 25 mM tris, 300 mM L-arginine-HCl, 360 mM urea, 48 mM GnHCl, 4 mM cystamine-2HCl, 1 mM L-cysteine, pH 9.0 for a period of 24 h at 4 °C with gentle stirring. Upon completion of the refolding period, the material was buffer exchanged into 20 mM tris, pH 8.0.

The first purification step was conducted using a Q Sepharose FF column (GE Healthcare, Piscataway, NJ) with a salt gradient from 10 mM tris, pH 8.0 to 10 mM tris, pH 8.0, 300 mM NaCl. The fractions were pooled based on SDS-PAGE analysis using a 4−20% tris-glycine nonreduced gel (Life Technologies, Carlsbad, CA), and the Q Sepharose pool was brought to 2 mM KH_2PO_4 and 0.5 mM $CaCl_2$ using 100 mM stock solutions. The second purification step took place using a CHT Ceramic Hydroxyapatite Type I column (BioRad, Hercules, CA) in a flowthrough manner with 20 mM tris, 2 mM KH_2PO_4, 0.5 mM $CaCl_2$, 160 mM NaCl, pH 8.0 as the mobile phase. The protein of interest was contained in the flowthrough and wash fractions. The protein concentration was determined by measuring its absorbance at 280 nm, and final product purity was assessed by SDS-PAGE on a 4−20% tris-glycine nonreduced gel. Endotoxin levels were measured using an Endosafe PTS LAL test system (Charles River, Wilmington, MA) ensuring that the sample was <0.5 EU/mg and protein identity was verified by MALDI/MS.

In order to prepare the sample for PEGylation, partial reduction was carried out with TCEP using a 1:2.2 molar ratio (FGF21:TCEP) at 25 °C for 30 min. The sample was then buffer exchanged into 10 mM imidazole, pH 7.5 using tangential flow filtration with a 3 kDa Centramate T-Series PES cassettes (Pall Corporation, Port Washington, NY) at 10 °C under a steady flow of N_2 to prevent premature oxidation of the sulfhydryls. The PEGylation reaction was carried out using a 1:2.5 molar ratio of FGF21 to maleimide-PEG (NOF America, Irvine, CA), at 25 °C for 30 min.

Post-PEGylation purification was conducted using a Q Sepharose HP column (GE Healthcare, Piscataway, NJ) with a salt gradient from 10 mM tris, pH 8.5 to 10 mM tris, 100 mM NaCl, pH 8.0. The fractions were pooled by SDS-PAGE using a 4−20% tris-glycine nonreduced gel, and the pooled sample was concentrated and buffer exchanged using tangential flow filtration with a 10 kDa Sartocon PES cassette (Sartorius, Gottingen, Germany) into a formulation buffer consisting of 10 mM tris, 9% sucrose, pH 8.5.

In Vitro Assay. The Elk1-luciferase reporter assay in human 293T cells was described previously.[24] Briefly, the 293T cells were stably expressing human βKlotho along with reporter constructs encoding 5xUAS luciferase and GAL4 DNA-binding domain fused to ELK1 (GAL4-Elk1). In this system, the luciferase activity is regulated by the endogenous phosphorylated extracellular signal-regulated kinase (ERK). The 293T stable cells were seeded at 1×10^5 cells/well on 96-well plates. On the following day, FGF21 proteins were added to the media, and the plates were incubated for six hours. Cells were then lysed to measure luciferase activity using the Bright-Glo luciferase assay system (Promega, Madison, MI) per the manufacturer's instructions. The EC_{50} values of FGF21 proteins were obtained by titrating proteins from as low as 10 pM to as high as 5 μM with 1:5 titrations to obtain full dose−response curve, and each dose was run in triplicate. The EC_{50} value was calculated using sigmoidal dose−response curve in GraphPad Prism software (GraphPad, La Jolla, CA).

In Vivo Studies. Mice were cared for in accordance with the *Guide for the Care and Use of Laboratory Animals*. All study

protocols were approved by the Institutional Animal Care and Use Committee (IACUC) of Amgen, Inc., or Covance Laboratories Inc. Upon receipt, mice were group-housed on a 12:12 h light:dark cycle in rooms at temperature between 20 and 26 °C and humidity between 30% and 70%, and had access to enrichment opportunities. Animals were assigned to treatment groups using a manual or computerized blocking procedure designed to achieve body weight balance with respect to treatment groups.

In Vivo Glucose Modulation. Male *ob*/*ob* mice were purchased at 6 weeks of age from Jackson Lab (Cat # 000697, Bar Harbor, ME). Mice had *ad libitum* access to a standard rodent chow diet (2020x Harlan Teklad) and drinking water. One week before the initiation of the experiment, mice were acclimated to handling, restraining, and weighing. On the day of the experiment, baseline blood glucose and body weight were measured. Mice were then randomized into groups to obtain comparable average blood glucose and body weight among the groups. Vehicle (10 mM Tris, 2.2% sucrose, 3.3% Sorbitol; pH 8.5) or pegylated FGF21 compounds at 1 mg/kg each were administered intraperitoneally (ip) into mice. Blood samples were obtained from the retro-orbital sinus vein of *ad libitum*-fed conscious mice at 6, 24, 72, 120, and 168 h after injection and blood glucose levels were measured with a One Touch Glucometer (LifeScan, Inc., Milpitas, CA). Body weights were measured at all time points except 6 h.

In Vivo Vacuole Formation Assessment. *Tissue Histology and Microscopic Evaluation.* Kidney, liver, and spleen were fixed in 10% neutral buffered formalin by immersion. Fixed tissues were dehydrated and embedded in paraffin. Tissues were sectioned at 4 μm, stained with hematoxylin and eosin (H&E), and multiple fields were examined at 40×, 200×, and 400× magnifications. The severity of vacuolar change in renal tubular epithelia was graded semiquantitatively using a tiered scale: no lesions (0), minimal (1+; rare, small vacuoles), mild (2+; modest numbers of ~3-μm-diameter vacuoles), moderate (3+; many ~3- to ~5-μm-diameter vacuoles), or marked (4+; myriad large; >5 μm diameter vacuoles). Assessors were blinded to the treatment group.

Mono-PEGylated FGF21. This study was designed to evaluate the potential for kidney vacuole induction of various human monopegylated FGF21 proteins when administered to female C57BL/6 mice at 10 mg/kg via subcutaneous injection once daily for seven days. Control animals were injected with vehicle (10 mM KHPO4, 150 mM NaCl, pH 8). Irradiated PicoLab Rodent Diet (LabTest) was supplied *ad libitum*, and animals were group-housed (3/cage). Clinical observations were made predose and 1−2 h postdose. Body weights were recorded at least once before dose initiation, on each dosing day before dose administration, and at the time of necropsy. Animals were necropsied the day following the last dose. Kidney and liver tissues were examined for PEG-induced vacuoles after staining with H&E.

Dual-PEGylated FGF21. This study was designed to evaluate the potential for kidney vacuole induction and effect on body weight of various human dual-pegylated FGF21 proteins administered to female C57BL16 mice via subcutaneous injection once weekly for 8 weeks. Mice were injected at 5 and 25 mg/kg with the dual-PEGylated FGF21 molecules along with the 20 kDa linear PEG-Control protein or vehicle only (10 mM Tris, 150 mM Sodium Chloride (NaCl), pH 8.0). Animals were 7 weeks of age at the initiation of treatment and multiple-housed (up to 5 per cage) in stainless steel cages unless individually housed to accommodate study procedures. Clinical observations were made predose and 1−2 h postdose. Body weights were measured at least once during the predose phase, prior to each dose administration, and on the third day post each dose administration. Animals were euthanized and the kidneys, liver, spleen, and gross lesions (if present) were collected and stored in 10% neutral buffered formalin. Tissues were processed and stained with H&E.

PEG Configuration Variants. This study was designed to evaluate the potential for kidney vacuole induction and effect on body weight of the PEG configuration variants when administered weekly via subcutaneous injection to female C57BL/6 mice (Charles River Laboratories, Portage MI) for four or eight weeks. An additional arm of the study included mice that were treated for eight weeks; however, they were then allowed to recover for an additional ten weeks prior to necropsy. Animals were 10 weeks of age at the time they were assigned to treatment groups. Five animals per group were given weekly injections of 25 mg/kg in a dose volume of 5 mL/kg. The control group received the control article [10 mM tris, pH 8.5, 8% sucrose (w/v)] only. Animals designated for the first interim necropsy were euthanized on Study Day 29. Animals designated for the terminal necropsy were euthanized on Study Day 57. The remaining animals/group were necropsied on Study Day 134 (Recovery Day 78).

Animals were multiple-housed (up to 3 per cage) in stainless steel cages unless individually housed to accommodate study procedures. Certified rodent diet #2016C (Harlan Teklad) was available *ad libitum*. Clinical observations were made predose and 1−2 h postdose. Body weights were measured at least once during the predose phase, prior to each dose administration, on the third day post each dose administration, weekly during the treatment-free phase, and at scheduled necropsies. Animals were fasted for at least 3 but no more than 5 h before necropsy (no access to food, water available). Animals were euthanized and the kidneys, liver, spleen, and gross lesions (if present) were collected and stored in 10% neutral buffered formalin. Tissues were processed and stained with H&E.

RESULTS

Mono-PEGylation of FGF21. A homology model of FGF21 bound to its receptor was generated using FGF19 as a template then manually positioning the resulting molecule in the dimeric FGF receptor 1 structure (Figure 1). The structural model was then used to identify the 14 sites in FGF21 that would be the most promising candidates to accept substitution with cysteine for site directed conjugation with polymer, while minimizing the risk of excessive interference with receptor binding. Furthermore, in order to probe the effect of PEGylation near the structurally unresolved C-terminus of FGF21, two sites were selected in this region based on primary amino acid sequence analysis. All but one of the 16 variants (H88C) was successfully expressed in *E. coli*, purified, and conjugated to a linear 20 kDa methoxy-PEG-maleimide (Li20) (data not shown).

The *in vitro* activity of all 15 PEG-conjugated variants was assessed using an Elk1-luciferase reporter assay in human 293T cells and compared to the activity of unconjugated FGF21 and FGF21 with a 20 kDa PEG conjugated to the amino terminus (Table 1). In this assay, 293T cells were stably transfected with human β-klotho and luciferase reporter genes which enables measurement of β-klotho-dependent FGFR downstream signaling. The *in vitro* activity of the amino terminally-PEGylated FGF21 (WT-NT-Li20, EC_{50} = 36.74 ± 6.05) was over 14-fold

dx.doi.org/10.1021/bc300603k | *Bioconjugate Chem.* 2013, 24, 915−925

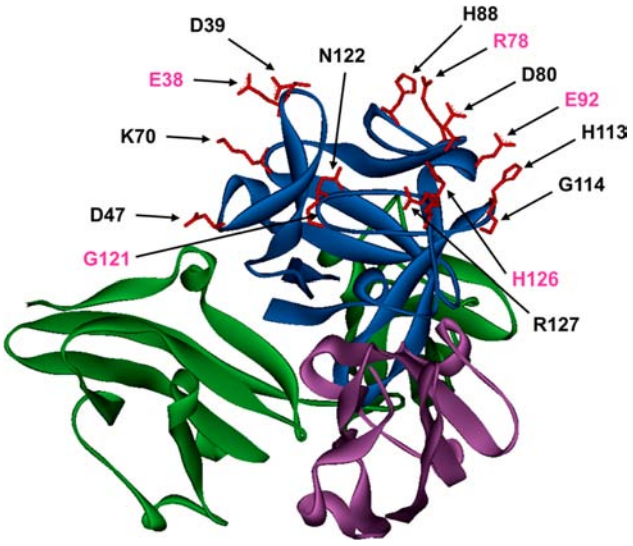

Figure 1. FGF21 homology model where FGF21 is blue and the green and purple structures are fragments of the FGFR1c dimer. Sites mutated to cysteine for targeted PEGylation are labeled and those used for the dual-PEGylation strategy are highlighted in magenta.

Table 1. *In Vitro* and *In Vivo* Properties of Mono-PEGylated FGF21[a]

Construct	EC_{50} (nM)	Kidney Vacuoles	Liver Vacuoles
Vehicle	N/A	0.0	0.0 ± 0.0
Control-Li20	N/A	3.7 ± 0.6	0.0 ± 0.0
WT	2.53 ± 0.41	N/A	N/A
WT-NT-Li20	36.74 ± 6.05	2.0 ± 0.0	0.0 ± 0.0
H126C−Li20	4.49 ± 0.92	2.3 ± 0.6	0.0 ± 0.0
D80C−Li20	4.61 ± 1.18	2.0 ± 0.0	0.0 ± 0.0
R78C−Li20	4.90 ± 0.71	2.3 ± 0.6	0.0 ± 0.0
G121C−Li20	6.02 ± 1.06	2.0 ± 0.0	0.0 ± 0.0
E38C−Li20	6.92 ± 1.36	2.0 ± 0.0	0.0 ± 0.0
R176C−Li20	7.85 ± 2.12	3.0 ± 0.0	0.0 ± 0.0
E92C−Li20	8.32 ± 1.24	2.7 ± 0.6	0.0 ± 0.0
N122C−Li20	9.15 ± 0.96	2.0 ± 0.0	0.0 ± 0.0
H113C−Li20	9.65 ± 0.61	2.6 ± 0.6	0.0 ± 0.0
R127C−Li20	9.99 ± 1.29	3.0 ± 0.0	0.0 ± 0.0
G114C−Li20	11.97 ± 1.08	2.7 ± 0.6	0.0 ± 0.0
D39C−Li20	13.05 ± 1.77	ND	ND
D47C−Li20	27.77 ± 2.32	3.0 ± 0.0	0.0 ± 0.0
K70C−Li20	34.52 ± 3.61	2.0 ± 0.0	0.0 ± 0.0
Y180C−Li20	287.10 ± 53.01	ND	ND
H88C−Li20	ND	ND	ND

[a]The Elk1-luciferase reporter assay in human 293T cells stably expressing human β-Klotho along with reporter constructs encoding 5xUAS luciferase and GAL4 DNA-binding domain fused to ELK1 (GAL4-Elk1) was described previously.[24] Error values are ± standard deviation. Three female C57BL/6 mice per group were given daily subcutaneous injections of 10 mg/kg for seven days. Animals were necropsied on the day following the last dose and the kidney and liver tissues were examined microscopically for vacuoles. The scoring criteria were as follows: 0 = no vacuoles, 1 = minimal vacuoles, 2 = mild vacuoles, 3 = moderate vacuoles, and 4 = marked vacuoles. Error values are ± standard deviation.

lower than that of the unconjugated FGF21 (WT, EC_{50} = 2.53 ± 0.41). Conjugation near the carboxy terminus also resulted in dramatic reduction in *in vitro* activity (Y180C−Li20, EC_{50} = 287.1 ± 53.01) In contrast, the *in vitro* activity of all other engineered variants was as good as or better than that of the amino-terminally PEGylated FGF21, and the activity of most of the engineered variants was within 4-fold of the unconjugated FGF21.

Mono-PEGylated FGF21 Vacuole Formation in Vivo. In order to evaluate the vacuole forming potential of the PEGylated FGF21 variants, mice were injected with 10 mg protein (not including PEG)/kg (mg/kg) with each molecule daily for seven days, then necropsied the day following the last dose. Kidney, liver, and spleen tissues were examined for PEG induced vacuoles after staining with H&E and scored from 0 to 4 based on severity (Figure 2). In this study, none of the PEGylated compounds

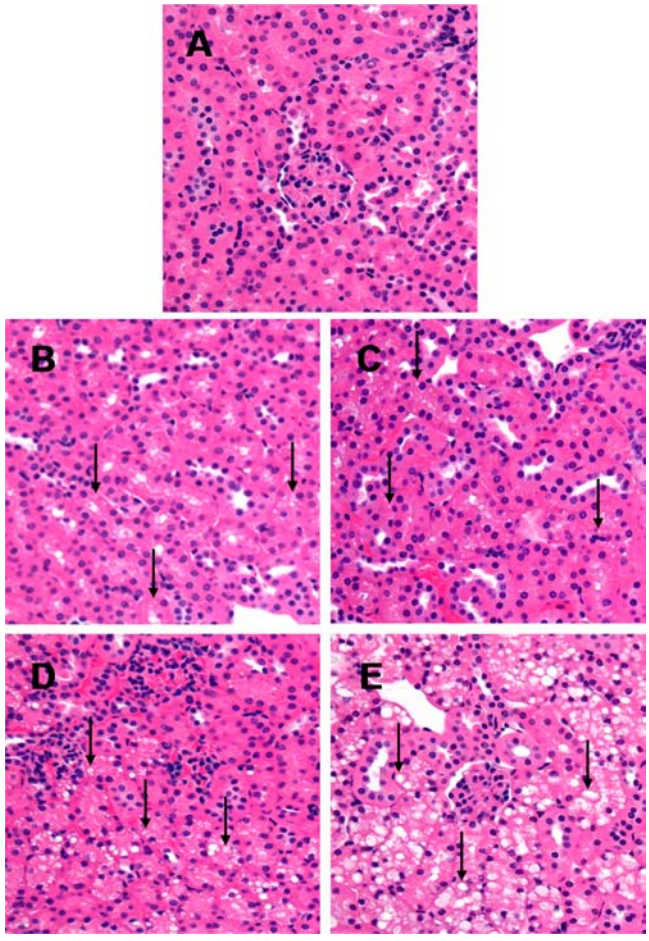

Figure 2. Representative examples of the severity scores for the vacuolar change in renal tubular epithelia: (A) no renal tubular vacuoles, (B) grade 1, (C) grade 2, (D) grade 3, and (E) grade 4. Vacuoles are shown by arrows. 400× magnification, H&E-stained kidney sections.

showed measurable vacuole formation in the liver or spleen; however, while not as severe as the PEG-Control, which is known to cause moderate to marked (grade 3−4) kidney vacuoles, all PEGylated variants showed mild to moderate (grade 2−3) vacuole formation in the kidneys. No large differences in kidney vacuole severity based on the site of PEGylation could be identified (Table 1), since all variants produced vacuoles in the grade 2−3 range; however, four of the grade 2 sites (E38C, K70C, G121C, and N122C) tended to cluster in one region on the surface of FGF21 (Figure 1).

Dual-PEGylation of FGF21. Six of the sixteen sites evaluated for mono-PEGylation of FGF21 (E38, R78, E92, G121, H126,

and R176) were chosen (Figure 1 magenta residues except R176 which is disordered in structure) for assessment as dual PEGylated molecules by creating double mutants of all possible combinations of those molecules, 15 in total. After purification, all molecules were conjugated with two linear 20 kDa methoxy-PEG-maleimides (2XLi20) and qualitatively evaluated for production efficiency (Table 2). The sites with the best

Table 2. Production Efficiency and *In Vitro* Activity of Dual-PEGylated FGF21[a]

Construct	Production Efficiency	EC_{50} (nM)
WT	N/A	2.53 ± 0.41
WT NT-Li20	++	36.74 ± 6.05
E38C/R78C-2XLi20	++	20.62 ± 2.25
G121C/H126C-2XLi20	+++	23.09 ± 2.39
R78C/E92C-2XLi20	+	26.48 ± 2.90
R78C/G121C-2XLi20	++	28.76 ± 2.86
R78C/H126C-2XLi20	+	29.91 ± 3.29
E92/H126C-2XLi20	++	34.29 ± 6.06
E38C/E92C-2XLi20	++	36.15 ± 3.68
E92C/R176C-2XLi20	++	42.55 ± 3.32
E38C/R176C-2XLi20	++	48.05 ± 3.92
E92C/G121C-2XLi20	+++	54.62 ± 4.5
E38C/G121C-2XLi20	+++	54.51 ± 9.34
R78C/R176C-2XLi20	+++	61.71 ± 7.30
E38C/H126C-2XLi20	+++	64.46 ± 6.67
G121C/R176C-2XLi20	+++	117.90 ± 10.20
H126C/R176C-2XLi20	+++	200.90 ± 25.80

[a]The overall dual-PEGylation efficiency was qualitatively assigned as follows: N/A = not applicable, + = poor, ++ = moderate, and +++ = very good. The Elk1-luciferase reporter assay in human 293T cells stably expressing human β-Klotho along with reporter constructs encoding 5xUAS luciferase and GAL4 DNA-binding domain fused to ELK1 (GAL4-Elk1) was described previously.[24] Error values are ± standard deviation.

PEGylation efficiency on average when combined with the other variants were G121C > H126C = R176C > E38C > E92C > R78C (based on ranking the average production efficiency score (1−3) of each mutation site). The PEGylated double variants were tested for *in vitro* activity using the ELK1-luciferase reporter assay in human 293T cells. The *in vitro* activity of the dual-PEGylated molecules was somewhat lower than that of their mono-PEGylated counterparts and the unconjugated protein; however, they were still quite potent with most maintaining an EC_{50} between 20 and 64 nM in the ELK1-luciferase assay (Table 2). The sites with the best *in vitro* activity on average, when combined with the other variants, were E92C > E38C > R78C > G121C > H126C > R176C (based on the average *in vitro* EC_{50} of each mutation site). The combination variants that showed both good PEGylation efficiency and good *in vitro* activity included E38C/R78C, G121C/H126C, R78C/G121C, E92C/H126C, E38C/E92C, E92C/R176C, E38/R176, E92C/G121C, E38C/G121C, R78C/H176C, and E38C/H126C.

Three of the double variants conjugated to two 20 kDa PEGs (2XLi20) that showed both good activity and good conjugation efficiency, and were PEGylated in a variety of locations (near the amino, middle, or carboxy regions) (E38C/R78C, E38C/H126C, and E92C/H126C) were examined for potency and vacuole formation in mice. All three of these dual-PEGylated molecules were very efficacious in lowering blood glucose levels in *ob/ob* mice for at least nine days after a single injection of 1 mg/kg (Figure 3).

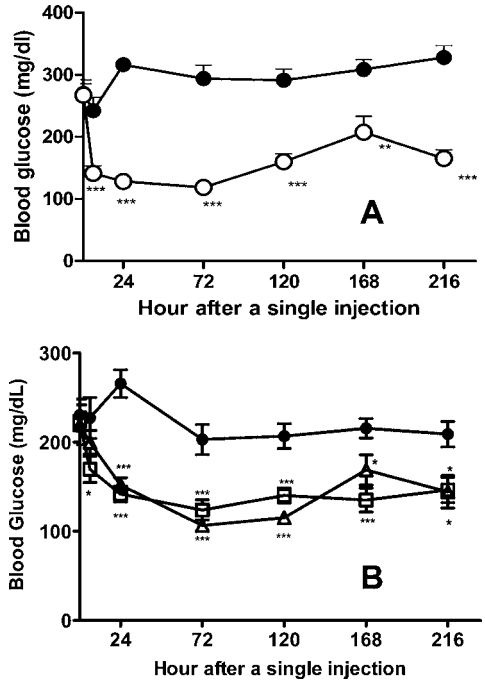

Figure 3. Dual PEGylated FGF21s caused a long-lasting blood glucose reduction in *ob/ob* mice following a single administration. (A) Effect of E38C/R78C-2xLi20 (○) or (B) E92C/H126C-2xLi20 (Δ) and E38C/H126C-2xLi20 (□) on blood glucose levels in *ob/ob* mice. 8−9-week-old *ob/ob* mice were administered intraperitoneally (ip) with vehicle (●) or indicated compound at 1 mg/kg. Blood glucose levels were measured at the indicated time points. All data are mean ± SEM, $n = 9-10$ animals per group, * $p < 0.05$, ** $p < 0.01$, *** $p < 0.001$ compared with vehicle at each time point.

Dual-PEGylated FGF21 Vacuole Formation *in Vivo*. Mice were injected at 5 and 25 mg/kg weekly for eight weeks with the dual-PEGylated FGF21 molecules along with the 20 kDa linear PEG-Control protein or vehicle only, and they were regularly monitored for body weight, then necropsied one week after the final dose to examine the kidneys, liver, and spleen for the presence of vacuoles. While all three PEGylated FGF21 molecules were significantly more efficacious than either vehicle or the PEG-Control at maintaining a lower body weight over the course of the study (Figure 4), the E38C/R78C variant performed slightly better at both 5 mg/kg and 25 mg/kg. Although none of the molecules produced liver or spleen vacuoles, all three molecules produced substantial kidney vacuoles at 25 mg/kg by termination of the study, but the severity was slightly less than the PEG-Control (Figure 5). However, at 5 mg/kg the E38C/R78C and E38C/H126C produced minimal kidney vacuoles that were substantially less severe than the PEG-Control, and the E92C/H126C molecule did not produce detectable vacuoles at the 5 mg/kg dose.

PEG Configuration Variants. In order to determine if the PEG configuration and/or PEGylation sites could affect vacuole formation, four different PEGs [linear 20 kDa (Li20) and 40 kDa (Li40) and branched 20 kDa (Br20) and 40 kDa (Br40)] were conjugated to three different FGF21 variants (R78C, E92C/H126C, and G121C/H126C) with either one PEG or two PEGs (2X) per protein to produced a total of six molecules (Figure 6). All product molecules were examined for uniformity and

dx.doi.org/10.1021/bc300603k | *Bioconjugate Chem.* 2013, 24, 915−925

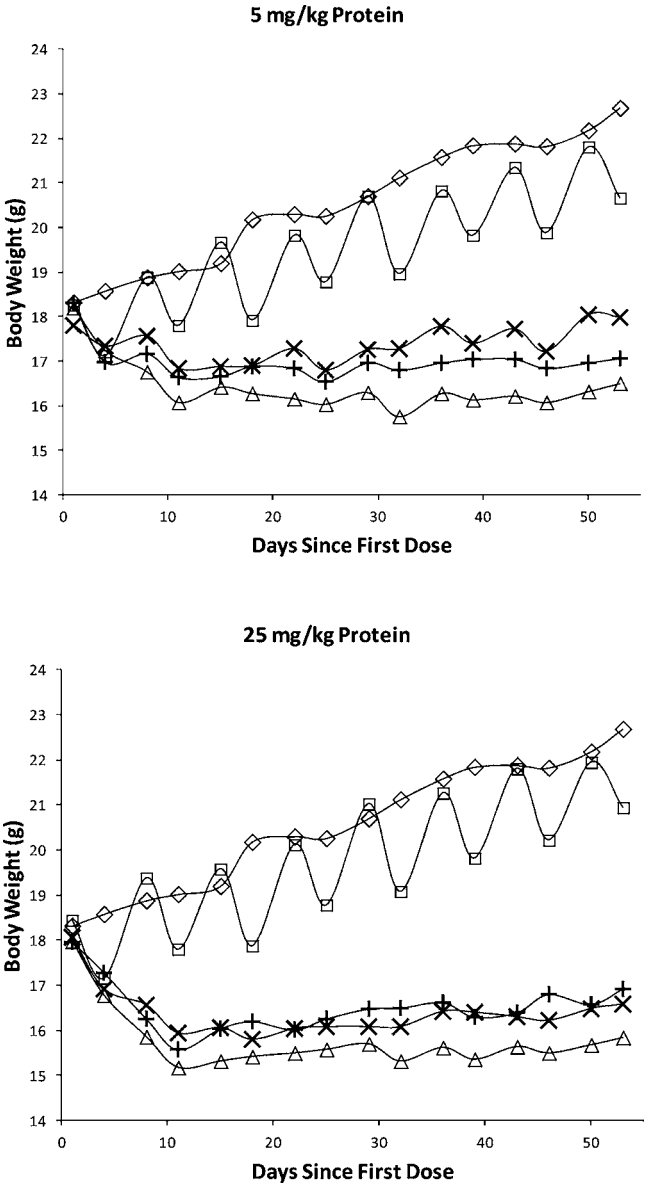

Figure 4. Body weight of C57BL/6 mice treated weekly with ◊ Vehicle, (□) Control-Li20, (Δ) FGF21(E38C/R78C)-2XLi20, (×) FGF21-(E38C/H126C)-2XLi20, and (+) FGF21(E92C/H126C)-2XLi20 for eight weeks at either 5 mg/kg or 25 mg/kg. There were five animals per study group.

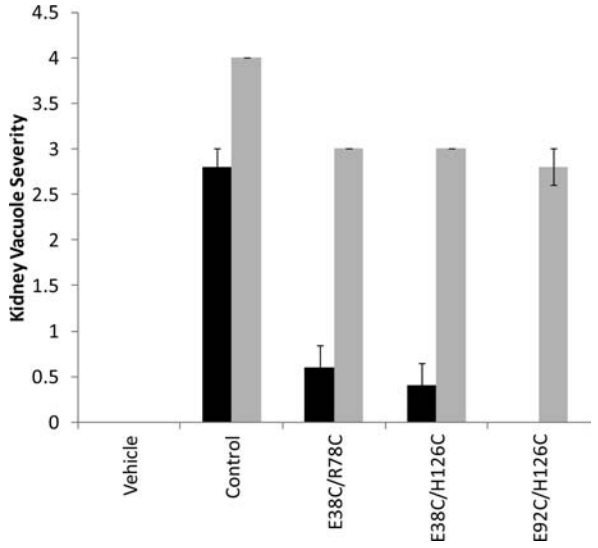

Figure 5. Five female C57BL/6 mice per group were given weekly subcutaneous injections of 5 (black bars) or 25 mg/kg (gray bars) for 8 weeks. Animals were necropsied on the week following the last dose and the kidney and liver were stained with hematoxylin and eosin and examined microscopically for vacuoles. The scoring criteria were as follows: 0 = no vacuoles, 1 = minimal vacuoles, 2 = mild vacuoles, 3 = moderate vacuoles, and 4 = marked vacuoles. There were five animals per study group and error bars are ± standard error of the mean.

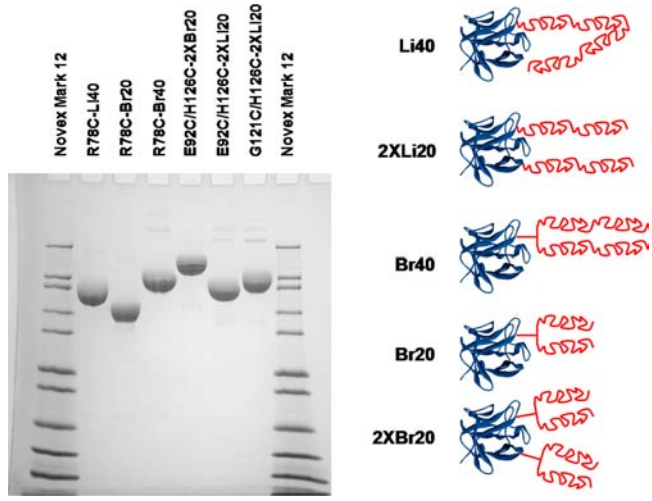

Figure 6. Purified conjugated products were analyzed by Coomassie blue stained SDS-PAGE using a 4−20% tris glycine gel. Molecular weight standards are Novex Mark 12. The cartoon figures illustrate the various PEG configurations of the six different molecules tested.

migration rates by Coomassie SDS-PAGE (Figure 6). The linear molecules migrate faster than the branched molecules (R78C−Li40 vs R78C−Br40 and E92C/H126C-2XLi20 vs E92C/H126C-2XBr20) and the E92C/H126C-2XLi20 molecule with more distant PEGylation sites in the primary sequence migrated faster than the G121C/H126C-2XLi20 with more proximal PEGylation sites. All six molecules were evaluated for *in vitro* activity using the Elk1-luciferase reporter assay in human 293T cells (Table 3). The mono-PEGylated molecules maintained activity (EC_{50} between 5.71 and 13.06 nM) comparable to the unconjugated FGF21 at 2.53 nM, but they did show decreasing activity correlated with more extended PEG configurations (Br20 > Br40 > Li40). The dual-linear PEGylated molecules also maintained a high level of activity (EC_{50} of 10.65 and 21.97 nM); however, the dual-branched PEGylated E92C/H126C molecule suffered an 82-fold decrease in activity (208.6 nM) compared to the unconjugated FGF21, and it lost almost 20-fold activity compared to its linear PEGylated counterpart. Four of the six PEGylated compounds were examined for their ability to lower blood glucose levels of *ob/ob* mice after a single injection of 1 mg/kg (Figure 7). All four molecules tested showed efficacy for at least five days *in vivo* after a single injection. In contrast to the difference in *in vitro* activity of the mono- and di-PEGylated molecules, no discernible pattern was detected in the *in vivo* efficacy on blood glucose level under the tested conditions, even for the E92C/H126C-2XBr20, which had substantially reduced *in vitro* activity compared to the other molecules.

dx.doi.org/10.1021/bc300603k | *Bioconjugate Chem.* 2013, 24, 915−925

Table 3. *In Vitro* Activity of Varied PEG Configurations of FGF21[a]

	EC_{50} (nM)
R78C−Br20	5.71 ± 0.37
R78C−Br40	8.49 ± 0.97
R78C−Li40	13.06 ± 1.33
G121C/H126C-2XLi20	21.97 ± 3.73
E92C/H126C-2XLi20	10.65 ± 0.86
E92C/H126C-2XBr20	208.6 ± 26.9

[a]Three mono-PEGylated and three dual-PEGylated FGF21 variants were assessed for *in vitro* activity using the Elk1-luciferase reporter assay in human 293T cells stably expressing human β-Klotho along with reporter constructs encoding 5xUAS luciferase and GAL4 DNA-binding domain fused to ELK1 (GAL4-Elk1) was described previously.[24] Error values are ± standard deviation.

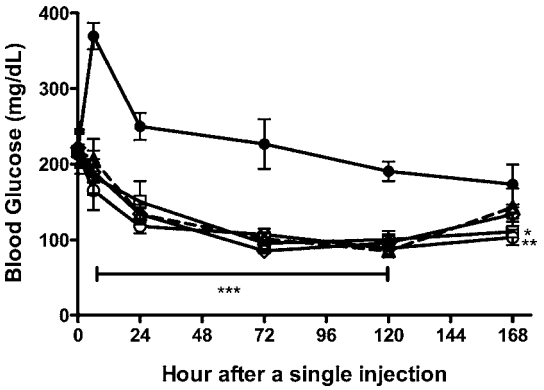

Figure 7. Glucose-lowering effect of branched PEGylated FGF21 in *ob/ob* mice following a single administration. 8−9 week old *ob/ob* mice were administered ip with vehicle (●) or E92C/H126C-2xLi20 (○, **), E92C/H126C-2xBr20 (Δ), R78C−Br20 (◊), R78C−Br40 (□, *) at 1 mg/kg. Blood glucose levels were measured at the indicated time points. All data are mean ± SEM, n = 9−10 animals per group, * $p < 0.05$, ** $p < 0.01$, *** $p < 0.001$ compared with vehicle at each time point.

PEG Configuration Variants and Vacuole Formation *in Vivo*. All six of the lead molecules were examined for efficacy and vacuole formation potential *in vivo* by treating mice weekly with 25 mg/kg for either four or eight weeks, monitoring body weights periodically during the study and conducting a necropsy one week after the last dose. An additional arm of the study included mice that were treated for eight weeks; however, they were then allowed to recover for an additional ten weeks prior to necropsy. The combined body weight data showed that all mono-PEGylated molecules were effective at maintaining a lower body weight during the course of the study, even ten weeks after dosing of the test molecules was terminated (Figure 8). However, of the dual PEGylated FGF21s, only the E92C/H126C-2XLi20 showed weight loss efficacy comparable to that of the mono-PEGylated molecules. The G121C/H126C-2XLi20 and E92C/H126C-2XBr20 variants showed marginal *in vivo* efficacy, falling between that of the negative control and the better molecules; however, even after dosing was terminated these molecules were superior to the vehicle control at long-term weight loss.

At the four or eight week necropsy, none of the animals showed measurable liver vacuoles; however, after four weeks of treatment, the R78C−Br20, R78C−Li40, and E92C/H126C-2XLi20 molecules showed mild to moderate kidney vacuole formation, while the R78C−Br40 and G121C/H126C-2XLi20 showed minimal vacuole formation, and the E92C/H126C-2XBr20 had no measurable vacuoles (Figure 9). After eight weeks of treatment R78C−Br20, R78C−Br40, and E92C/H126C-2XLi20 all showed increased kidney vacuoles, while the G121C/H126C-2XLi20 and E92C/H126C-2XBr20 had minimal vacuoles and did not show a significant increase from week four to week eight. After the ten week washout period, the three strongest vacuole forming molecules (R78C−Br20, R78C−Li40, and E92C/H126C-2XLi20) all showed a noticeable decrease in kidney vacuoles; however, the variants with minimal to mild vacuoles (R78C−Br40, G121C/H126C-2XLi20, and E92C/H126C-2XBr20) did not show a significant decrease after the 10 week recovery phase. Splenic vacuoles were not present with any of the test articles after four weeks treatment; however, they did appear after eight weeks of treatment in the R78C−Br40 (mild), R78C−Li40 (minimal), and G121C/H126C-2XLi20 (minimal) treatment groups. After a ten week recovery period with no treatment, the splenic vacuoles were substantially reduced in the R78C−Br40 and G121C/H126C-2XLi20 groups, but not the R78C−Li40 group.

DISCUSSION

FGF21 is being widely investigated as a treatment for type II diabetes, but the native protein has poor pharmacokinetic characteristics and would require very frequent injections to impart a biological effect. PEGylation is a well-known means of extending the circulating half-life of therapeutic proteins; however, conjugation of PEG to proteins often results in substantially reduced activity due to steric interference between the therapeutic protein and its target caused by the necessarily bulky PEG. Furthermore, PEGylated proteins often induce vacuoles in the kidney when administered frequently and/or at high dose levels, which could be particularly problematic considering the renal issues often associated with the diabetic target patient population of this potential therapeutic.

PEGs used for conjugation are typically of MW ≥ 5 kD and are unlikely to be metabolized to any significant degree. Instead, clearance is largely through glomerular filtration and excretion in the urine and/or uptake by phagocytes, depending on the size of the combined PEG-biomolecule construct.[21] The cellular uptake of the PEG conjugates produces clear cytoplasmic vacuoles, which have been described at multiple sites in rodents, dogs, pigs, and nonhuman primates. Vacuole formation is thought to arise mainly from endocytotic sequestration of PEG-linked proteins within lysosomes,[20] although binding of PEG to the polar heads of membrane phospholipids has also been posited based on in vitro experiments using endothelial cells.[25] The intralysosomal proteins are then digested,[20,26] but the lack of mammalian etherases capable of degrading PEG results in the gradual accumulation of insoluble, hygroscopic PEG within engorged lysosomes.[20]

The most commonly affected cell types are renal tubular epithelium[20] and resident visceral macrophages. For example, Cimzia (approved by the FDA in 2008 for chronic administration to control Crohn's disease; http://www.emea.europa.eu/humandocs/PDFs/EPAR/cimzia/H-740-RAR-en.pdf) caused cytoplasmic vacuoles in cells (mainly macrophages) at the injection site as well as in multiple organs (adrenal, cervix, choroid plexus, lymph nodes, spleen, and uterus) in monkeys and rats. Similarly, vacuoles were observed in lymph nodes and spleens, most likely in macrophages, in toxicity studies in rats treated with Somavert (approved by the FDA in 2003 for chronic treatment of acromegaly; http://www.accessdata.fda.gov/drugsatfda_docs/nda/2003/21106_Somavert_Pharmr_P2.pdf).

dx.doi.org/10.1021/bc300603k | *Bioconjugate Chem.* 2013, 24, 915−925

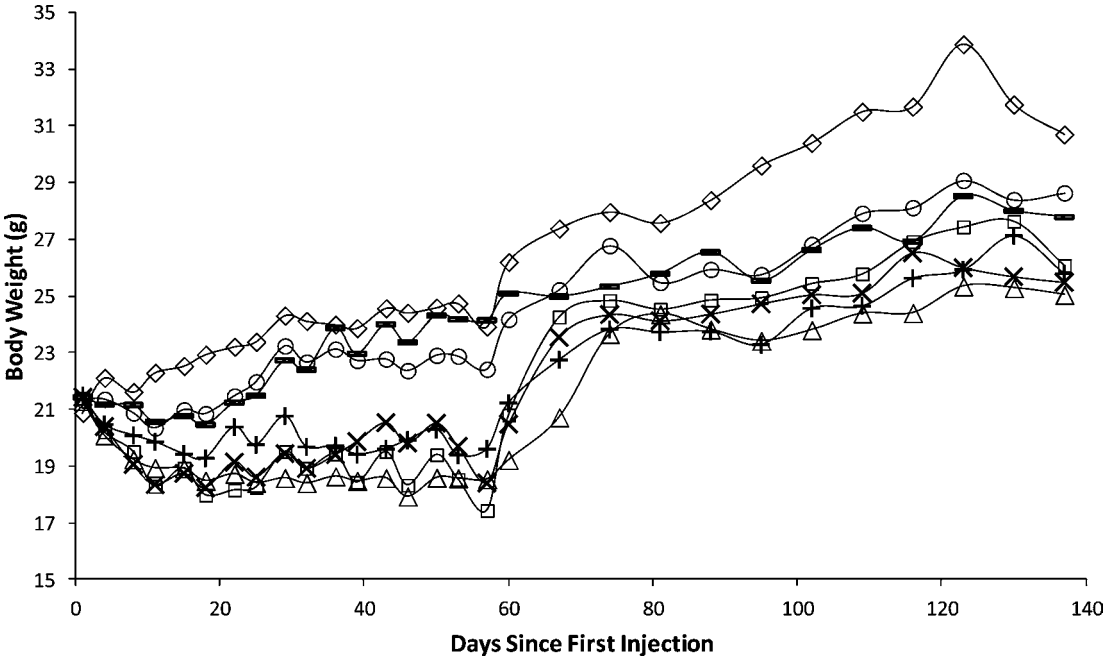

Figure 8. Body weight of mice treated weekly with 25 mg/kg for up to eight weeks followed by a 3-month recovery period: (◊) Vehicle, (□) FGF21(R78C)-Br20, (Δ) FGF21(R78C)-Br40, (×) FGF21(G121C/H126C)-Li40, (-) FGF21(G121C/H126C)-2XLi20, (○) FGF21(E92C/H126C)-2XBr20, and (+) FGF21(E92C/H126C)-2XLi20. There were at least five animals per study group.

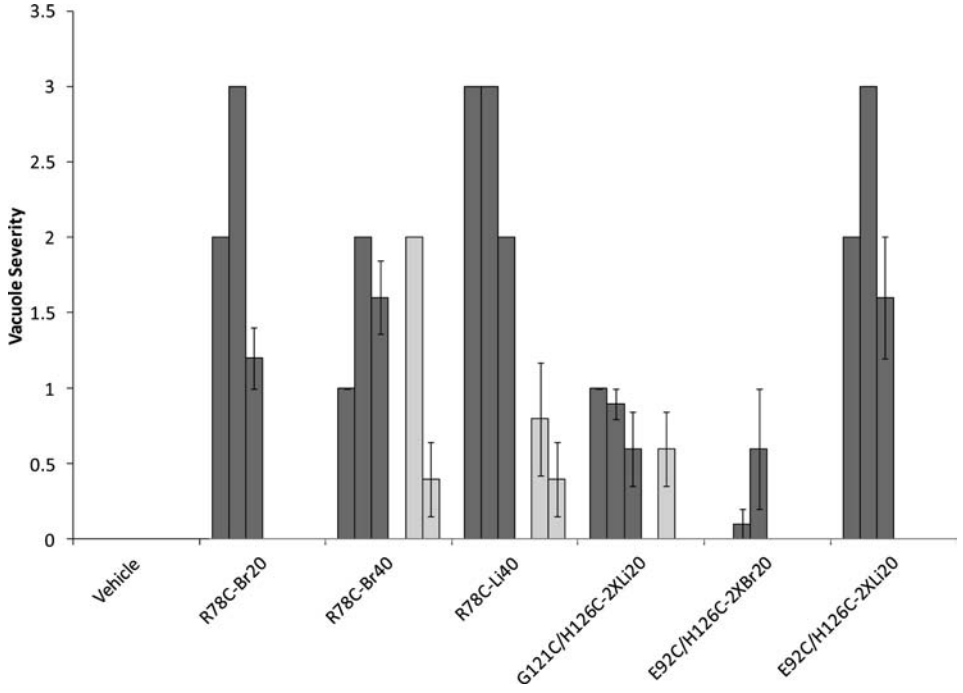

Figure 9. Five female C57BL/6 mice per group were given weekly subcutaneous injections of 25 mg/kg for 4 or 8 weeks. Animals were necropsied on the week following the last dose and the kidney and liver tissue samples were stained with hematoxylin and eosin and examined microscopically for vacuoles. One additional group was given weekly doses for 8 weeks, but then allowed to recover for an additional 10 weeks prior to necropsy. The scoring criteria were as follows: 0 = no vacuoles, 1 = minimal vacuoles, 2 = mild vacuoles, 3 = moderate vacuoles, and 4 = marked vacuoles. The dark gray bars are for the kidney samples in the following order: week 5, week 9, and week 19. The light gray bars are for the spleen samples in the following order: week 5, week 9, and week 19 (note all week 5 samples were negative, so no bars are showing). Error bars are ± standard deviation.

Published reports[20] and regulatory documents for PEG-linked human therapeutics (http://www.emea.europa.eu/humandocs/PDFs/EPAR/cimzia/H-740-RAR-en.pdf) indicate that partial recovery occurs for both renal tubular epithelium and macrophages. Recovery is thought to occur as a result of epithelial cell turnover,[20] although the contribution of extrusion of PEG-containing lysosomes cannot be excluded.[27] The extended period of time required for recovery is consistent with the long lifespan of differentiated renal tubule epithelial cells[28] and supports the contention that cell turnover is the primary means of recovery.

The vacuole-producing capacity of PEG-conjugated biomolecules diminish as the PEG side chains increase in size,[20,26] number, or complexity (i.e., branching).[26] The proposed mechanism for this hierarchy is that larger numbers of side chains, longer side chains, and/or branched side chains increase the hydrodynamic radius of the pegylated molecule, thereby reducing its ability to pass through the filtration pores in the renal glomerulus.[26] Despite the presence of PEG-induced vacuoles in renal proximal tubules, assessment of renal function by clinical chemistry and urinalyses has not revealed altered function in vivo, nor have PEG-induced vacuoles been shown to cause cytotoxicity in kidneys.[20] Further, treatment with PEG-conjugated biomolecules that are known to produce vacuoles primarily in macrophages (e.g., Cimzia [http://www.emea.europa.eu/humandocs/PDFs/EPAR/cimzia/H-740-RAR-en.pdf] and Somavert [http://www.accessdata.fda.gov/drugsatfda_docs/nda/2003/21-106_Somavert_Pharmr_P2.pdf]) has not been linked to an increased incidence of hepatic or renal disease related to PEG accumulation, either during clinical trials or postmarket monitoring.

Although data cited above give no indication that PEG-induced vacuoles are cause for concern in normally functioning kidneys, observations in patients with impaired kidneys suggest that concern related to the renal effects of PEG may be warranted in some patient populations. The concern surrounding PEG-induced renal effects on patients with impaired renal function was described by the FDA pharmacology/toxicology reviewer for Somavert (approved by the FDA in 2003 for chronic treatment of acromegaly). The reviewer comments on the renal effects of Somavert and states, "...The renal effects are most likely due to the PEG covalently bonded to B2036. This may not pose any threat to healthy acromegalic patients but in individuals with reduced renal function, the impact of repeated administration of B2036-PEG should not be ignored..." (http://www.accessdata.fda.gov/drugsatfda_docs/nda/2003/21106_Somavert_Pharmr_P1.pdf). Adding to the concern regarding functional significance of PEG-conjugate-induced vacuoles are observations that other agents known to induce formation of vacuoles in epithelium of renal proximal tubules, such as hydroxyethylstarch (HES),[29] mannitol, and sucrose,[30] have been associated with functional and sometimes morphologic indications of adverse renal effects.

In order to address these issues, we investigated a wide array of PEGylation sites on FGF21 as well as several PEG configurations and PEGylation strategies. Using a homology model of FGF21 bound to its primary receptor, we identified 14 sites on the surface of the protein that appeared to be promising locations for site directed PEGylation while maintaining activity. After mutating these sites to cysteine and employing targeted PEGylation using linear 20 kDa PEG-maleimide, we found that most variants maintained *in vitro* activity similar to that of the wild type molecule; however, all these molecules showed significant kidney vacuole formation when dosed daily at high level for a week (70 times the 1 mg/kg weekly dose that produces strong efficacy in the glucose model). The site of PEGylation does not make a large difference with regard to vacuole formation potential, since all variants tested produced mild to moderate vacuoles, but four out of five of the molecules with mild vacuoles were associated with sites clustered together, indicating there may be a modest positional effect on vacuologenesis.

In order to investigate the possibility that PEGylating more than one site at a time might both improve the pharmacokinetic profile and reduce the vacuole formation potential, six of the fourteen single site variants were produced in all possible combinations of two for dual PEGylation. Production of dual PEGylated molecules is more complex than single PEGylated proteins because conjugation of the first PEG often interferes with conjugation of the second PEG, likely due to steric interference, and the additional engineered cysteines can compete with the native disulfide bond formation in FGF21. To address this we compared the production efficiency of the dual PEGylated molecules and found those residues closer to the carboxy terminus tended to dual PEGylate better (G121C, H126C, and R176C) and those closer to the middle tended to fare worse (E92C, R78C, and K70C). It is possible that the proximity of the two native cysteines (C76 and C94) that normally form a disulfide bond in FGF21 interfere with the efficient production of middle PEGylated molecules. While the E92C and R78C containing double variants were more difficult to produce, they also tended to produce molecules with the highest *in vitro* activity. The more amino-terminal E38C containing variants were an exception in that they were intermediate in production efficiency, but demonstrated very good *in vitro* activity. The G121C and H126C containing double mutants resulted in intermediate *in vitro* activity levels but were very efficiently produced; therefore, with FGF21 there is some trade-off between optimum *in vitro* activity and efficient production. The three dual-PEGylated variants chosen for the vacuole study were all very efficacious *in vivo*, lowering the blood glucose level in *ob/ob* mice for at least nine days in spite of possessing diminished *in vitro* activity compared to their unPEGylated counterpart (less than one day *in vivo*; data not shown). As frequently observed with PEGylated proteins, it is likely that the improvement in pharmacokinetics more than compensates for the diminished *in vitro* activity. Following daily treatment of mice for one week with three of the dual-PEGylated variants, all three molecules showed a profound and long-lasting weight reduction in the mice lasting over 50 days. Since there was no major difference between the 5 and 25 mg/kg groups, it is likely that a dose significantly lower than 5 mg/kg would be efficacious, which is consistent with the observation that molecules with approximately 20-fold difference in *in vitro* activity show similar efficacy in the blood glucose model at only 1 mg/kg. The dual PEGylated molecules were significantly less prone to form vacuoles than the mono-PEGylated proteins, scoring only 0 to 0.6 at the 5 mg/kg dose compared to scores of 2.0 to 3.0 at 10 mg/kg for the mono-PEGylated FGF21s (the PEG load for both these studies was equivalent, since the dual-PEGylated FGF21s contain twice the PEG load per unit mass of protein). However, at the high dose of 25 mg/kg, all three dual PEGylated molecules showed moderate vacuole formation with average scores from 2.8 to 3.0.

Due to the high risk for renal problems in the target patient population, an even lower vacuole forming potential was deemed desirable; therefore, various PEG configurations were examined. We compared linear 40 kDa (Li40), branched 20 kDa (Br20), branched 40 kDa (Br40), dual linear 20 kDa (2XLi20), and dual branched 20 kDa (2XBr20) configurations, and we explored the effect of conjugation site proximity in the dual PEGylated molecules comparing E92C/H126C (33 residues separation) to G121C/H126C 2XLi20 (four residues separation). Examination of the *in vitro* activity of all six molecules showed that all but one maintained excellent activity; however, the E92C/H126C-2XBr20 FGF21 was nearly 20-fold less active than its linear PEG counterpart. It is possible that either the E92 and/or H126 sites are exceptionally sensitive to the presence of a branched PEG, but both locations will accommodate a linear PEG with

only minimal degradation of *in vitro* activity. Of the four variants examined for ability to lower glucose levels in *ob/ob* mice, two showed efficacy for at least five days and the other two showed efficacy for at least seven days. The two that showed slightly lower efficacy had either the smallest PEG (R78C−Li20K), likely resulting in less favorable pharmacokinetics, or had the lowest *in vitro* activity (E92C/H126C-2XBr20) by 10- to 20-fold compared to the others.

During the long-term 25 mg/kg weekly injection study, all mono-PEGylated molecules and E92C/H126C-2XLi20 displayed a strong weight loss effect; however, the E92C/H126C-2XBr20 and G121C/H126C-2XLi20 had noticeably lower potency *in vivo*. The lower efficacy of the E92C/H126C-2XBr20 compared to the E92C/H126C-2XLi20 was not unexpected, since it has nearly 20-fold lower activity *in vitro,* and it was in the group of the lowest efficacy *in vivo* in the *ob/ob* glucose lowering model. The lower efficacy of the G121C/H126C-2XLi20 compared to E92C/H126C-2XLi20 indicates that the E92C site is superior to the G121C site for weight loss in the dual-PEG format even though their *in vitro* potencies were comparable (2-fold difference), which demonstrates the importance of PEG configuration. After drug administration was terminated, the body weight of animals treated with the four more potent molecules increased substantially over a ten day period to become similar to those of animals treated with the less potent compounds; however, even 80 days after the last dose, the body weights of all the treatment groups were substantially lower than those of the controls, demonstrating a long lasting effect of the compounds on body weight. This also suggests there may be a bimodal mechanism (short duration and long duration) for weight loss.

The long-term high weekly dose study demonstrated a significant difference in vacuole-forming potential dependent on the configuration of the PEG with regard to the therapeutic protein. The kidney vacuole level was significantly higher in the Br20 group compared to the Br40 group, indicating that larger branched PEGs reduce vacuole formation. Furthermore the Li40 group had more severe vacuoles than the Br40 group, indicating that branched PEG also lowers vacuole formation compared to a linear PEG. Compared to linear PEG, the E92C/H126C-2XLi20 molecule formed vacuoles at a level similar to that of the mono-PEGylated molecules indicating that distributing the PEG along the surface does not provide an automatic advantage compared to a branched PEG counterpart (R78C−Br40). Surprisingly, vacuole formation was lower in the G121C/H126C-2XLi20 compared to the mono-PEGylated molecules with the same mass of PEG (Li40 or Br40). The superiority of this molecule compared to its close cousin that differs only in the location of one of the two PEG units (E92C/H126C-2XLi20) may be due to a more branched-like PEG structure resulting from the proximity of the PEGs, or it may be due to a superiority of the G121C position compared to E92C or a combination of both. The lack of difference observed with the E92C/H126C-2XLi20 and R78C−Br40 suggests the improvement is more likely due to superiority of the G121C position. Furthermore, the mono-PEGylated kidney vacuole study supports at least a partial role for the superiority of G121C (score 2.0) compared to E92C (score 2.7). The E92C/H126C-2XBr20 FGF21 forms nearly undetectable levels of kidney vacuoles, again demonstrating the superiority of branched PEG when compared to the linear PEG version of this molecule. It is possible the exceptional performance of this molecule is due to it essentially being a branched-branched PEG, since two branched PEGs are on separate locations of FGF21.

Engineering PEGylated molecules that are highly potent *in vivo*, have an acceptable level of vacuole formation rate and are efficient to produce is an iterative empirical process; however, a strategy based on structural information of the target and its receptor can be employed to more rapidly identify the optimal location for PEG attachment. Furthermore, some general observations with PEG vacuole formation potentials can be combined with the structure activity relationship to more efficiently identify configurations that possess the desired properties.

AUTHOR INFORMATION

Corresponding Author

*E-mail: kennethw@amgen.com.

Author Contributions

J.X. and J.B. contributed equally to this manuscript.

Notes

The authors declare no competing financial interest.

ACKNOWLEDGMENTS

We would like to acknowledge Brad Bolen, Colin Gegg, Randy Hecht, Luke Li, Steven Vonderfect, and Lily Yin for their contributions to the FGF21 project.

ABBREVIATIONS

FGF, fibroblast growth factor; PEG, polyethylene glycol; GLP1, glucagon like peptide 1; FGFR, fibroblast growth factor receptor; LDL, low density lipoprotein; HDL, high density lipoprotein

REFERENCES

(1) Brown, J. B., Nichols, G. .A., and Perry, A. (2004) The burden of treatment failure in type 2 diabetes. *Diabetes Care 27*, 1535−40.

(2) Itoh, N. (2010) Hormone-like (endocrine) Fgfs: their evolutionary history and roles in development, metabolism, and disease. *Cell Tissue Res. 342*, 1−11.

(3) Fukumoto, S. (2008) Actions and mode of actions of FGF19 subfamily members. *Endocr. J. 55*, 23−31.

(4) Holt, J. A., Luo, G., Billin, A. N., Bisi, J., McNeill, Y. Y., Kozarsky, K. F., Donahee, M., Wang, D. Y., Mansfield, T. A., Kliewer, S. A., Goodwin, B., and Jones, S. A. (2003) Definition of a novel growth factor-dependent signal cascade for the suppression of bile acid biosynthesis. *Genes Dev. 17*, 1581−91.

(5) Nabeshima, Y. (2010) Regulation of calcium homeostasis by alpha-Klotho and FGF23. *Clin. Calcium 20*, 1677−85.

(6) Kharitonenkov, A., and Shanafelt, A. B. (2008) Fibroblast growth factor-21 as a therapeutic agent for metabolic diseases. *BioDrugs 22*, 37−44.

(7) Fon Tacer, K., Bookout, A. L., Ding, X., Kurosu, H., John, G. B., Wang, L., Goetz, R., Mohammadi, M., Kuro-o, M., Mangelsdorf, D. J., and Kliewer, S. A. (2010) Research resource: Comprehensive expression atlas of the fibroblast growth factor system in adult mouse. *Mol. Endocrinol. 24*, 2050−64.

(8) Kurosu, H., Choi, M., Ogawa, Y., Dickson, A. S., Goetz, R., Eliseenkova, A. V., Mohammadi, M., Rosenblatt, K. P., Kliewer, S. A., and Kuro-o, M. (2007) Tissue-specific expression of beta-Klotho and fibroblast growth factor (FGF) receptor isoforms determines metabolic activity of FGF19 and FGF21. *J. Biol. Chem. 282*, 26687−95.

(9) Kharitonenkov, A., Shiyanova, T. L., Koester, A., Ford, A. M., Micanovic, R., Galbreath, E. J., Sandusky, G. E., Hammond, L. J., Moyers, J. S., Owens, R. A., Gromada, J., Brozinick, J. T., Hawkins, E. D., Wroblewski, V. J., Li, D. S., Mehrbod, F., Jaskunas, S. R., and Shanafelt,

A. B. (2005) FGF-21 as a novel metabolic regulator. *J. Clin. Invest. 115*, 1627−35.
(10) Wente, W., Efanov, A. M., Brenner, M., Kharitonenkov, A., Koster, A., Sandusky, G. E., Sewing, S., Treinies, I., Zitzer, H., and Gromada, J. (2006) Fibroblast growth factor-21 improves pancreatic beta-cell function and survival by activation of extracellular signal-regulated kinase 1/2 and Akt signaling pathways. *Diabetes 55*, 2470−8.
(11) Xu, J., Stanislaus, S., Chinookoswong, N., Lau, Y. Y., Hager, T., Patel, J., Ge, H., Weiszmann, J., Lu, S. C., Graham, M., Busby, J., Hecht, R., Li, Y. S., Li, Y., Lindberg, R., and Veniant, M. M. (2009) Acute glucose-lowering and insulin-sensitizing action of FGF21 in insulin-resistant mouse models–association with liver and adipose tissue effects. *Am. J. Physiol. Endocrinol. Metab. 297*, E1105−14.
(12) Xu, J., Lloyd, D. J., Hale, C., Stanislaus, S., Chen, M., Sivits, G., Vonderfecht, S., Hecht, R., Li, Y. S., Lindberg, R. A., Chen, J. L., Jung, D. Y., Zhang, Z., Ko, H. J., Kim, J. K., and Veniant, M. M. (2009) Fibroblast growth factor 21 reverses hepatic steatosis, increases energy expenditure, and improves insulin sensitivity in diet-induced obese mice. *Diabetes 58*, 250−9.
(13) Kharitonenkov, A., Wroblewski, V. J., Koester, A., Chen, Y. F., Clutinger, C. K., Tigno, X. T., Hansen, B. C., Shanafelt, A. B., and Etgen, G. J. (2007) The metabolic state of diabetic monkeys is regulated by fibroblast growth factor-21. *Endocrinology 148*, 774−81.
(14) Coskun, T., Bina, H. A., Schneider, M. A., Dunbar, J. D., Hu, C. C., Chen, Y., Moller, D. E., and Kharitonenkov, A. (2008) Fibroblast growth factor 21 corrects obesity in mice. *Endocrinology 149*, 6018−27.
(15) Hecht, R., L., Y., Sun, J., Belouski, E., Hall, M., Hager, T., Yie, J., Wang, W., Winters, D., Smith, S., Spahr, C., Tam, L. T., Shen, Z., Stanislaus, S., Chinookoswong, N., Lau, Y., Sickmier, A., Michaels, M. L., Boone, T., Véniant, M. M., and Xu, J. (2012) Rationale-based engineering of a potent long-acting FGF21 analog for the treatment of type 2 diabetes. *PLOS One 7* (11), e49345.
(16) Mu, J., Pinkstaff, J., Li, Z., Skidmore, L., Li, N., Myler, H., Dallas-Yang, Q., Putnam, A.-M., Yao, J., Bussell, S., Wu, M., Norman, T. C., Rodriguez, C. G., Kimmel, B., Metzger, J. M., Manibusan, Al., Lee, D., Zaller, D. M., Zhang, B. B., DiMarchi, R. D., Berger, J. P., and Axelrod, D. W. (2012) FGF21 Analogues of Sustained Action Enabled by Orthogonal Biosynthesis Demonstrate Enhanced Antidiabetic Pharmacology in Rodents. *Diabetes 61* (2), 505−512.
(17) Harris, J. M., and Chess, R. B. (2003) Effect of pegylation on pharmaceuticals. *Nat. Rev. Drug Discovery 2*, 214−221.
(18) Jain, A., and Jain, S. K. (2008) PEGylation: an approach for drug delivery. *Crit. Rev. Ther. Drug Carrier Syst. 25* (5), 403−447.
(19) Veronese, F. M., and Mero, A. (2008) The impact of PEGylation on biological therapies. *BioDrugs 22* (5), 315−329.
(20) Bendele, A., Seely, J., Richey, C., Sennello, G., and Shopp, G. (1998) Short communication: renal tubular vacuolation in animals treated with polyethylene-glycol-conjugated proteins. *Toxicol. Sci. 42*, 152−157.
(21) Webster, R., Didier, E., Harris, P., Seigel, N., Stadler, J., Tilbury, L., and Smith, D. (2007) PEGylated proteins: Evaluation of their safety in the absence of definitive metabolism studies. *Drug Metab. Dispos. 35*, 9−16.
(22) Fiser, A., and Sali, A. (2003) Modeler: generation and refinement of homology-based protein structure models. *Methods Enzymol. 374*, 461−491.
(23) Emsley, P., and Cowtan, K. Coot (2004) Model-building tools for molecular graphics. *Acta Crystallogr., Sect. D: Biol. Crystallogr. 60*, 2126−2132.
(24) Yie, J., Hecht, R., Patel, J., Stevens, J., Wang, W., Hawkins, N., Steavenson, S., Smith, S., Winters, D., Fisher, S., Cai, L., Belouski, E., Chen, C., Michaels, M. L., Li, Y. S., Lindberg, R., Wang, M., Véniant, M., and Xu, J. (2009) FGF21 N- and C-termini play different roles in receptor interaction and activation. *FEBS Lett. 583*, 19−24.
(25) Beckman, J. S., Minor, R. L., Jr, White, C. W., Repine, J. E., Rosen, G. M., and Freeman, B. A. (1998) Superoxide dismutase and catalase conjugated to polyethylene glycol increases endothelial enzyme activity and oxidant resistance. *J. Biol. Chem. 263*, 6884−6892.
(26) Bolon, B., Faust, J., Storm, N., et al. (2001) Cytoplasmic vacuoles in renal tubular epithelium of mice given polyethylene glycol (PEG) conjugated protein are reduced by altering PEG size and conformation [abstract]. *Toxicologist 60*, 376.
(27) Brandt, E. J., Elliott, R. W., and Swank, R. T. (1975) Defective lysosomal enzyme secretion if kidneys of Chediak-Higashi (beige) mice. *J. Cell Biol. 67*, 774−788.
(28) Vogetseder, A., Karadiniz, A., Kaissling, B., and Le Hir, M. (2005) Tubular cell proliferation in the healthy rat kidney. *Histochem. Cell Biol. 124*, 97−104.
(29) Boldt, J., Brosch, C., Ducke, M., Papsdorf, M., and Lehmann, A. (2007) Influence of volume therapy with a modern hydroxyethystarch preparation on kidney function in cardiac surgery patients with compromised renal function: a comparison with human albumin. *Crit. Care Med. 35* (12), 2740−2746.
(30) Dickenmann, M., Oetti, T., and Mihatsch, M. J. (2008) Osmotic nephrosis: acute kidney injury with accumulation of proximal tubular lysosomes due to administration of exogenous solutes. *Am. J. Kidney Dis. 51*, 491−503.